

Journal of Composite Materials

<http://jcm.sagepub.com>

Constrained Layer Damping of Initially Stressed Composite Beams Using Finite Elements

V.S. Rao, B.V. Sankar and C.T. Sun
Journal of Composite Materials 1992; 26; 1752
DOI: 10.1177/002199839202601204

The online version of this article can be found at:
<http://jcm.sagepub.com/cgi/content/abstract/26/12/1752>

Published by:



<http://www.sagepublications.com>

On behalf of:

American Society for Composites

Additional services and information for *Journal of Composite Materials* can be found at:

Email Alerts: <http://jcm.sagepub.com/cgi/alerts>

Subscriptions: <http://jcm.sagepub.com/subscriptions>

Reprints: <http://www.sagepub.com/journalsReprints.nav>

Permissions: <http://www.sagepub.co.uk/journalsPermissions.nav>

Citations <http://jcm.sagepub.com/cgi/content/refs/26/12/1752>

Constrained Layer Damping of Initially Stressed Composite Beams Using Finite Elements

V. S. RAO,¹ B. V. SANKAR AND C. T. SUN
*Department of Aerospace Engineering, Mechanics
and Engineering Science
University of Florida
231 Aero Bldg.
Gainesville, FL 32611-2031*

(Received June 25, 1990)
(Revised December 20, 1991)

ABSTRACT: This paper presents the development of an efficient finite element model for the analysis of laminated composite beams treated by a constrained viscoelastic layer. The formulation presented includes the ability to model a structure about preloaded configurations. Since most of the damping ability is due to the shearing of the viscoelastic layer, the model is designed to represent this aspect accurately. An offset beam, shear-deformable element, which is specially suited for modeling such laminated beams is presented. The viscoelastic layer is modeled by using two-dimensional plane finite elements which are compatible with the beam elements. In case of a structure with initial load, the final equations are linearized so that first increment of motion, the part due to the initial load is linear, and the second, the part due to the dynamic load is linearized. System damping and tip displacement are compared with existing approximate results and experimental data whenever possible. Results confirm that dynamic response is substantially improved by use of such damping treatments, and give some useful information regarding designing a structure for high damping using constrained damping treatments.

KEY WORDS: damping, composite materials, constrained viscoelastic materials, finite element method, initial stresses.

INTRODUCTION

HIGH DAMPING IN a structure can often improve performance in a dynamic load environment. Material damping of conventional metallic materials such as carbon steel and aluminum alloys is too low (usually less than 0.001) to satisfy the design requirements. For laminated composites, damping can be improved by

¹Presently with Shell Development Company, Houston, Texas.

choosing a proper fiber aspect ratio composites, fiber orientations and stacking sequences [1–3]. However, for most polymer matrix composites, loss factors are still limited to around 0.02 after all usable methods are employed to increase damping ability.

Damping in undamaged fiber reinforced polymer composites is primarily due to the viscoelastic behavior of the constituent materials. Viscoelastic damping is believed to be almost entirely developed due to shear dissipation and practically independent of dilatation. In general, the effectiveness of the damping performance of a viscoelastically damped structure can be increased by increasing the extent of shear deformation of the viscoelastic layer. In the case of constrained viscoelastic damping treatments, the disparity in stiffness of the composite structure and the constraining layer with the viscoelastic layer (see Figure 1) force the viscoelastic layer to deform in shear. In order to design effective damping treatments, accurate and efficient methods are required to analyze and estimate the overall damping ability of composite structures subjected to such damping treatments.

Analysis of initially stressed, damped structures to control resonant noise and vibration problems is important for designing components like structural panels in aircraft and spacecraft, and helicopter rotor blades. Prestress in a structure affects the stiffness of a structure which modifies the dynamic characteristics of the structure. In this paper, the effect of axial prestress on the flexural behavior is studied by specializing previously developed finite elements [4] to include the ability to model structures about prestressed states. The finite element implementation of the modal strain energy method [5], and the direct frequency response method [6] are used to analyze the free and forced vibration characteristics of a prestressed composite beam. The modal strain energy method is modified to take into account the initially stressed state of the structure. Damping in the system is represented by using the complex stiffness approach which derives from the elastic-viscoelastic correspondence principle. In this approach, the real modulus of classical elasticity is replaced by its complex viscoelastic counterpart. The real part is called the storage modulus, and the complex part the loss modulus.

Results of the effect of different lengths treatment on the damping ability of laminated composite beams is presented. Results showing the effect of prestress on the modal parameters of the beam are also presented. Experimental results are presented wherever possible to compare with and validate the analytical results.

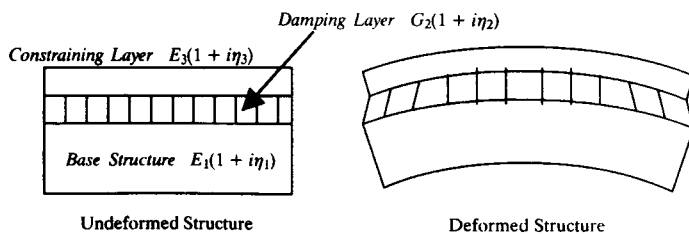


Figure 1. Constrained layer damping of a beam.

FORMULATION OF FINITE ELEMENT EQUATION FOR COMPOSITE STRUCTURES WITH PRESTRESS

Finite element equations were developed by using the principle of incremental virtual work [7]. In the current problem, a sequence of two motions is considered to include the effect of a static preload. The first increment is due to the application of a known static preload, and the second increment is due to a dynamic increment superposed on this known static configuration. The total Lagrangian definition of motion is used where all static and kinematic variables are referred back to the natural undeformed configuration. The formulation models a stress stiffening effect which causes a change in the stiffness within the element. Physically, it represents the coupling between inplane and transverse deflections within the structure, and is modeled as a higher order effect. The stress stiffening matrix is represented by an additional stiffness matrix, $[K_s]$. The mechanism is often used in flexible structures to increase the lateral load carrying capacity of the member.

Consider a body whose initial configuration is denoted by C_0 and in which Cartesian coordinates X_i are assigned to a point in the structure. After subsequent deformation of the body, the position of the same particle is given by x_i , in its current configuration C_1 . This state is the intermediate state caused by a known preload. State C_2 is the final state to be determined after the final increment of load is applied. The configuration in the final state is actually evaluated by calculating the incremental solution between the states C_1 and C_2 and updating the C_1 state deformation.

The principle of virtual work [7] in state α is written using indicial notation as,

$$\int_{V_0} (\alpha T_{ij} \delta_\alpha E_{ij} + {}_0 \rho \alpha \ddot{u}_i) dV = \int_{V_0} \alpha f_i \delta u_i dV + \int_{\partial V_0} \alpha t_i \delta u_i dA \quad (1)$$

where

T_{ij} = Piola-Kirchoff stress tensor (2nd kind)

E_{ij} = Green's strain tensor

f_i = body forces

t_i = surface traction

u_i = displacement

\ddot{u}_i = acceleration

The left subscript denotes the configuration, and all kinematic and force variables are referred to the initial undeformed configuration. Variables with no left subscripts are incremental quantities. The forces due to the state of motion are included as body forces in the D'Alembert sense.

By subtracting the virtual work expressions for the state 1 from the expression for state 2, simplifying further, and assuming a linear relation between the increments of Lagrangian stress and strain ($T_{ij} = D_{ijkl} E_{kl}$), the statement of incre-

mental virtual work can be expressed entirely in terms of displacement variables as,

$$\int_{v_0} (D_{ijkl} E_{kl} \delta E_{ij} + {}_1T_{ij} \delta \zeta_{ij} + {}_0Q \ddot{u}_i \delta u_i) dV = \int_{v_0} f_i \delta u_i dV + \int_{a_{v_0}} t_i \delta u_i dA \quad (2)$$

The equation is linearized by assuming linear expressions, e_{ij} , for the nonlinear incremental strains E_{ij} . ${}_1T_{ij}$ is stress at the intermediate state C_1 and is calculated by solving the static problem due to the known preload. For the loadings considered in this paper, a further assumption is made that the volume of the body does not change, so that the measures of stress are approximately the same and therefore the Cauchy stress at the prestressed state is used to calculate the stress stiffening matrix. The assumed displacement fields, shape functions of the offset beam element and the calculation of the stiffness matrix are presented in the next section. The offset nature of the element allows for the nodes to be displaced a chosen distance from the neutral surface, and makes it possible to model a laminated beam treated by a constrained viscoelastic layer by just two layers of nodes. The geometric stiffness matrix which accounts for the coupling between inplane and transverse displacements is derived from the second term in the principle of incremental virtual work. The derivation of the geometric stiffness matrix and the mass matrix is similar to the derivation of the conventional stiffness matrix, and is not presented.

FINITE ELEMENT MODEL AND CALCULATION OF STIFFNESS MATRIX OF THE LAMINATED BEAM ELEMENT

The offset beam element, and a typical finite element mesh used for modeling the three layer sandwich are shown in Figures 2 and 3 respectively. The base structure and constraining layer were modeled by using a specially developed three-node, seven-degree-of-freedom, offset beam element. The element is shear-deformable, which is significant for fiber-reinforced composites. A key feature of this element is its ability to account for coupling between stretching and bending deformations. This allows for the beam nodes to be offset to one surface of the beam, coincident with the nodes of the adjoining element. The viscoelastic core is modeled by using a rectangular plane stress element that is compatible with the offset beam element. The calculation of the elastic stiffness matrix of the offset beam element is discussed below.

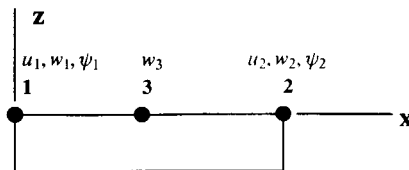


Figure 2. Offset beam element with nodes on the top side.

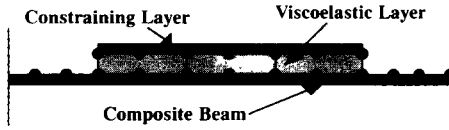


Figure 3. Finite element model of a beam with constrained layer damping treatment.

Offset Beam Element

The element stiffness matrix of the offset beam element shown in Figure 2 is formulated as follows. The assumed displacement field is

$$u(x, z) = u_0 - z\psi(x) \quad w(x, z) = w(x) \quad \psi(x, z) = \psi(x) \quad (3)$$

u_0 and ψ are defined by using linear interpolation functions,

$$u(x) = [(1 - x/L_e)x/L_e][u_1 u_2]^T \quad \psi(x) = [(1 - x/L_e)x/L_e][\psi_1 \psi_2]^T \quad (4)$$

where u_1, u_2, ψ_1 and ψ_2 are corresponding nodal displacements. The transverse displacement w is defined by using quadratic interpolation functions,

$$w = \begin{bmatrix} (1 - 3x/L_e + 2x^2/L_e^2) \\ 4(x/L_e - x^2/L_e^2) \\ (-x/L_e + 2x^2/L_e^2) \end{bmatrix}^T \begin{Bmatrix} w_1^e \\ w_2^e \\ w_3^e \end{Bmatrix} \quad (5)$$

where w_1^e, w_2^e and w_3^e are nodal displacements.

Strains are derived from displacements by using the strain-displacement relations,

$$\begin{pmatrix} \epsilon_{xx} \\ \epsilon_{xz} \end{pmatrix} = \begin{pmatrix} u_{0,x} \\ w_{0,x} - \Psi \end{pmatrix} - z \begin{pmatrix} \psi_{,x} \\ 0 \end{pmatrix} \quad (6)$$

The stress-strain relation is

$$\begin{pmatrix} \sigma_{xx} \\ \sigma_{xz} \end{pmatrix} = \begin{bmatrix} \bar{Q} & 0 \\ 0 & \bar{Q}_s \end{bmatrix} \begin{pmatrix} \epsilon_{xx} \\ \epsilon_{xz} \end{pmatrix} \quad (7)$$

After substituting Equations (6) and (7), the first term in the virtual work expression can be written in matrix form as,

$$\int_{V_0} C_{ijrs} \epsilon_{rs} \delta \epsilon_{rs} dV = \int_A \{\delta E\} [G] \{E\} dA \quad (8)$$

where the vector $\{E\}$ and the matrix $[G]$ are

$$\{E\} = \begin{Bmatrix} u_{o,x} \\ w_{o,x} - \psi \\ \psi_{,x} \end{Bmatrix} \tag{9}$$

$$[G] = \begin{bmatrix} A & B & 0 \\ B & D & 0 \\ 0 & 0 & F \end{bmatrix} \tag{10}$$

$$A, B, D, F = \int_{z_0-h/2}^{z_0+h/2} \bar{Q}, z\bar{Q}, z^2\bar{Q}, \bar{Q}_s dz$$

The element stiffness matrix $[K^e]$ is calculated by substituting the assumed displacement field given in Equations (4) and (5) in Equation (8). The first term in the incremental virtual work expression reduces to

$$\int_{V_0} C_{ijrs} \epsilon_{rs} \delta \epsilon_{rs} dV = \int_A \{\delta E\} [G] \{E\} dA = \{\delta u^e\} [K^e] \{u^e\} \tag{11}$$

The entries of $[K^e]$ are calculated by using the appropriate substitutions required in Equation (11). The geometric stiffness matrix is calculated from the second term in the virtual work expression. As can be seen from the term, the geometric stiffness matrix depends on the intermediate stress state which is calculated by performing a static analysis due to the preload.

Modeling and Solution Techniques

As mentioned before the base structure was modeled by using the three-node shear-deformable beam element. Typically, 20 elements are used to model the beam. Very large aspect ratios are common for elements used to model the viscoelastic core. Values as high as 5000:1 have been used successfully, and are sometimes even necessary, since the viscoelastic core is only 0.000127 mm thick [5]. Aspect ratios up to 200:1 were used in the present study. To validate this formulation, several calculations were made to determine natural frequencies and tip displacement of simple systems, closed form solutions to which are easily derived.

The loss factor was evaluated by using direct frequency-response (DFR) technique and the modal strain energy method. In the DFR method, a forced vibration at a known frequency is considered. System displacements are obtained by

solving a system of complex-valued linear equations. This technique is not very efficient, and is used only to verify the results from the modal strain energy method. Both the techniques are discussed in greater detail in the next section.

CALCULATION OF LOSS FACTOR

Damping is an important consideration in several applications and better results are often achieved from damping by design. For low levels of damping, the choice of method is influenced more by efficiency than by difference in numerical result. Two different methods to evaluate system loss factor are discussed briefly, the direct frequency response method and the modal strain energy method [5,6]. In both methods the overall damping of the structure is calculated from the independent properties of the constituent materials that form the composite structure.

In the direct frequency response method, a forced vibration over a range of frequencies is considered and a theoretical response spectrum is generated for which the overall damping of the system is calculated. For the forced vibration problem, the objective is to predict the linear, damped, steady-state response of structures about a linear preloaded equilibrium configuration. Since the complex modulus approach is used, the governing differential equations are complex. Following the finite element discretization procedure, the equations governing the time dependent response of a prestressed body is obtained as

$$\{[K] + [K_G]\}\{U\} + [M]\{\dot{U}\} = \{F\}$$

where

- $[K]$ = global stiffness matrix (complex)
- $[K_g]$ = global stress stiffening matrix
- $[M]$ = global mass matrix
- $\{U\}$ = global displacement vector (complex)
- $\{\dot{U}\}$ = global acceleration vector (complex)

An excitation force, harmonic in time, is considered; that is

$$F = fe^{i\omega t}$$

where ω is the forcing frequency, t the time and $i = (-1)^{1/2}$. The response due to the applied force is assumed to be harmonic and vibrating at the excitation frequency. The equation of motion reduces to

$$\{[K] + [K_G]\}\{U\} - \omega^2[M]\{U\} = \{f\}$$

The matrix on the left-hand side is called the displacement impedance matrix. For each frequency of excitation, the displacement per unit applied force is calculated by solving the system of complex-valued simultaneous linear equations and the response function is thereby generated. Loss factor is calculated from the

generated response spectrum by using the half-power-bandwidth technique, or from the real part of the spectrum as shown in Figure 4b.

The second technique is based on an eigenvalue problem which derives from setting the forcing terms to zero; that is,

$$\{[K] + [K_G]\}\{U\} = \omega^2[M]\{U\}$$

The natural frequencies and mode shapes are calculated about the initially stressed state for the undamped system. The stiffness matrix and the corresponding nodal displacements are real since only the real eigenvalue problem is solved. Modal damping is calculated by this technique by using the modal strain energy method. This technique is valid only for systems with relatively small levels of damping where the mode shapes and frequencies of the damped and the undamped structure are similar, therefore, causing the fraction of strain energy stored in each element to also be similar. The system loss factor is calculated as the weighted sum of the loss factor of each individual element, where the weighting factor is the fraction of the strain energy stored in the element. Due to the stiffening effect of the prestress a significant amount of energy will be stored in the beam due to an apparent stiffness increase. The weighting factors have to be modified to account for this increase in stored energy since the dissipated energy per cycle does not change very much. Loss factor for vibration about prestressed configuration is calculated by

$$\eta = \sum_{i=1}^{i=n} \eta_i E_i^m \bigg/ \sum_{i=1}^{i=n} E_i$$

where

n = total number of elements

η_i = loss factor of the i^{th} element

E_i^m = elastic strain energy stored in i^{th} element calculated as $1/2\{u\}^T[k]\{u\}$

E_i = sum of elastic strain energy and strain energy due to preload in the i^{th} element calculated as $1/2\{u\}^T[k + k_g]\{u\}$

The modal strain energy based method is the most popular because of the computational efficiency of the method. A variation of the modal strain energy method has been used [8] where the displacement impedance matrix, discussed under the direct frequency response method, is solved over a range of frequencies to locate the resonant frequency. The deflected shape at resonance of the damped structure is used to calculate the strain energy fractions stored in the element. Accuracy of this result depends on obvious factors and the computational benefits of the method discussed earlier are lost. Even though an assumption of small damping is made in the formulation, accurate results have been reported for core loss factors as high as 1.

Experimental Procedure

The most common methods used to measure damping are the free vibration decay method, the resonant dwell method, the hysteresis loop method and the frequency-response technique. For all experimental measurements of loss factor presented in this paper, the frequency response technique [9] was used. This technique offers potential for rapid non-destructive evaluation of materials and structures. In this technique, the specimen is excited impulsively with a controlled-impact hammer with a force transducer attached to its head. The specimen response is sensed by a non-contacting eddy current proximity probe. The signals from the force transducer and the motion transducer are sent to a Fast Fourier Transform (FFT) analyzer which displays the frequency response spectrum. A block diagram of the instrumentation required is shown in Figure 4a. By analyzing the resonant peaks for a particular mode, the loss factor, a measure of damping, is obtained from the real part of the response spectrum as explained in Figure 4b.

One feature of this technique is that the excitation level is accurately controlled, therefore, the amplitude of vibration of the specimen can be kept to a minimum (thereby reducing air damping to a minimum). Also, the response function, which is identical in shape to the transfer function after ensemble averaging can be used for damping measurements. This result has been verified for impulsive excitation only.

RESULTS AND DISCUSSION

Structural damping with and without the damping treatment was evaluated experimentally and by using a finite element approach. Results of the effects of different parameters such as length of the treatment and location of the treatment on the overall damping of the composite system are discussed. Three different unidirectional glass/epoxy composite beams were tested, and the average measured loss factor was used as input data to the finite element model. The same specimens were tested after application of damping tape. Each specimen was

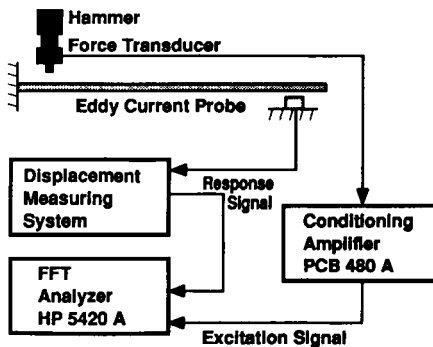


Figure 4a. Flexural vibration apparatus.

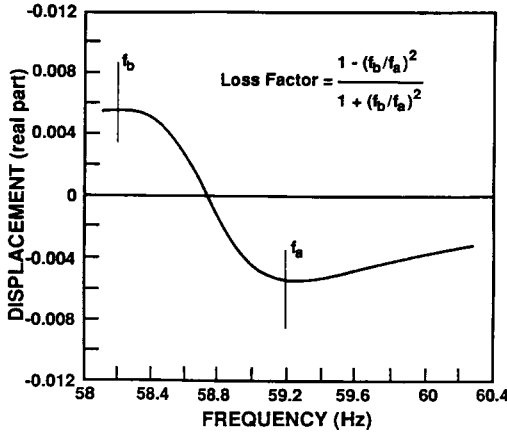


Figure 4b. Real part of the response spectrum.

made of glass/ epoxy ($V_f = 50\%$), and was 203 mm long, 3.6 mm thick and 25 mm wide. The damping tape used was SJ2052X, a constrained viscoelastic damping tape manufactured by 3M. Figures 2–3 shows the offset beam element and a typical finite element mesh of taped composite beam.

The specimen dimensions for the results of Figures 5 and 6 are the same as those given for the bare beam. The damping tape of appropriate length is applied to cover the required fraction of beam length completely. Figure 5 shows finite element and experimental results for the variation of loss factor with tape length. The result shows the existence of a tape length less than the length of the beam for which the damping is optimal. The result is significant and has also been observed by Plunkett and Lee [10]. This result confirms that the shear deformation of the viscoelastic layer is primary source of energy dissipation. Comparing the trend observed for mode 2 with the trend for mode 1 suggests that applying the damping material to the point of high strain energy density yields the best result. Figure 6 shows the variation of tip displacement in mm/N for different lengths of damping treatment. A significant reduction in vibration amplitude at resonance can be seen. A clear optimum length for the damping treatment is seen from the damping curves, but the tip displacement variation does not show the same clear result. This is because displacement is function of both damping and stiffness.

Figures 7–9 show the effect of preload on damping and frequency for different lengths of damping tape. In all cases the damping tape is applied starting at the fixed end of the beam. Frequency dependent properties of the damping material at room temperature were used in the calculations. The specimen used is a five ply graphite epoxy beam of stacking sequence [90/90/0/90/90], length 0.2032 m, width 0.01905 m, and thickness of 0.00064 m. For the static part of the loading, the beam is fixed with an axial load acting at the free end and for the dynamic

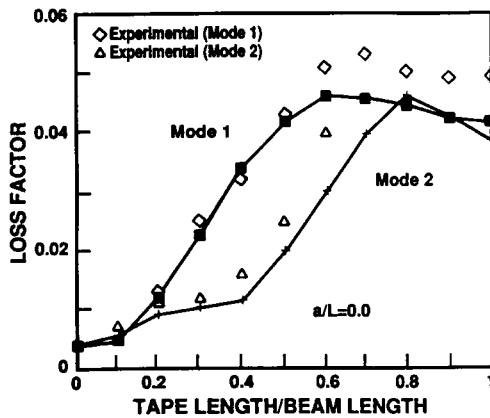


Figure 5. Analytical and experimental results (glass/epoxy base beam).

part of the loading the beam is fixed at both ends. In all the cases damping decreases with increasing preload for each of the first three modes but the stiffness of the structure has increased at the same time. Decreased loss factor, therefore, does not necessarily result in increased vibration amplitude (see Figure 10) since dynamic displacement depends on both stiffness and damping.

Figure 11 shows the results of loss factor and frequency of fully taped and bare beams for different preloads compared with experimental results of Mantena [11]. At the preload of 45 N, the analytical and experimental first mode frequencies significantly differ. At other preloads the results of both frequency and loss factor are in good agreement before any failure is initiated. Failure is believed to be initiated at the point at which the loss factor shows an increase with increasing preload in the experimental result. At high preloads the difference between finite ele-

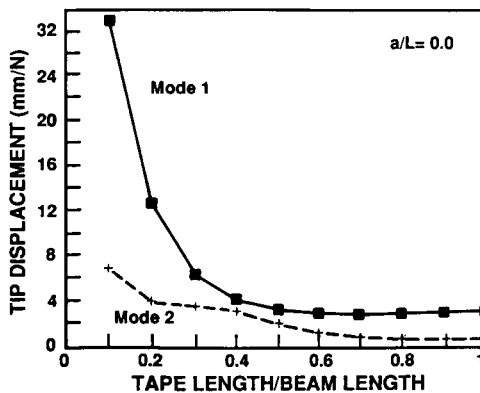


Figure 6. Variation of tip displacement (glass/epoxy base beam).

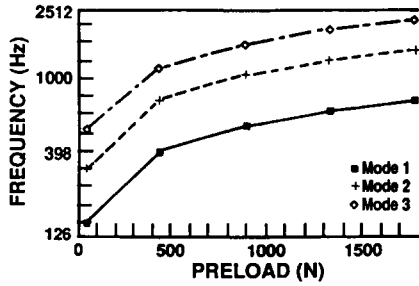
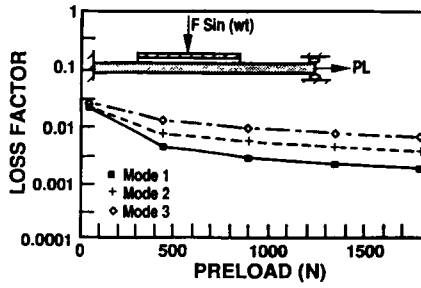


Figure 7. Variation of loss factor and frequency with preload (20% tapered from the root).

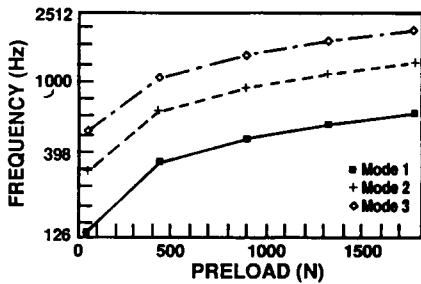
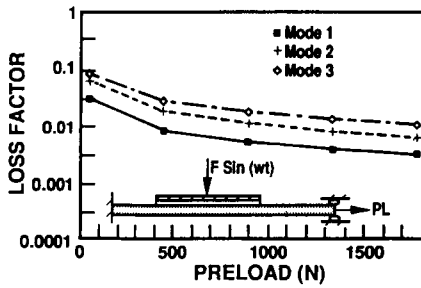


Figure 8. Variation of loss factor and frequency with preload (40% tapered from the root).

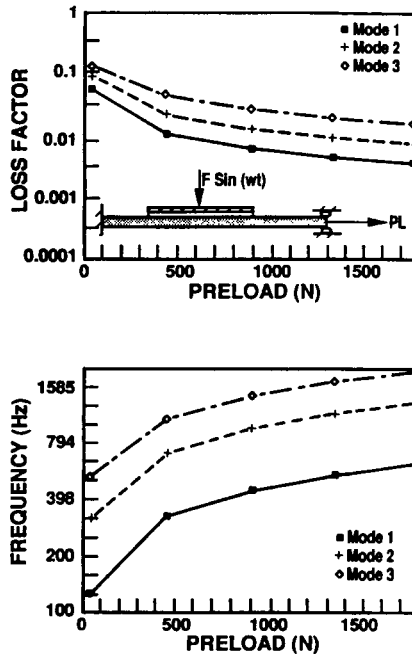


Figure 9. Variation of loss factor and frequency with preload (60% taped from the root).

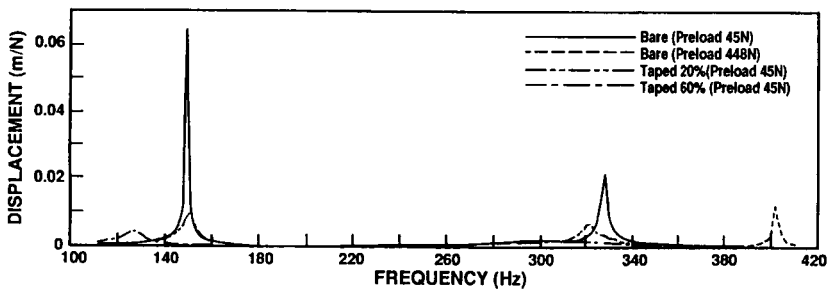


Figure 10. Response spectra for different preloads and tape lengths.

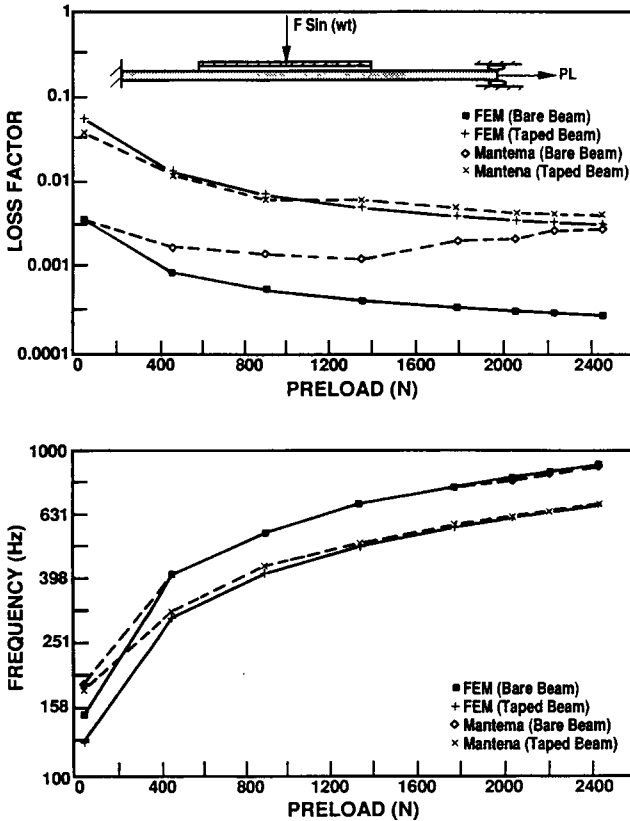


Figure 11. Variation of loss factor and frequency with preload (100% taped from the root).

ment results and experimentally measured is due to the problems associated with measurement of small levels of damping.

Results in Figure 5 suggest that application of the damping material to the points of high strain energy density in the structure would yield best results. This result can be seen by comparing the effect of different lengths of damping tape on loss factors of the three modes. Stress stiffening can have a significant effect on the location of damping material as it redistributes the strain energy distribution and should be considered in the design of a structure for maximum damping by using constrained layer damping treatments.

ACKNOWLEDGEMENT

This work is sponsored by the Army Research Office and monitored by Dr. Gary L. Anderson under contract No. DAAL03-88-k0013.

REFERENCES

1. Gibson, R. F., S. K. Chaturvedi and C. T. Sun. 1982. "Complex Moduli of Aligned Discontinuous Fiber Reinforced Polymer Composites," *Journal of Material Science*, 17:3499-3509.
2. Sun, C. T., J. K. Wu and R. F. Gibson. 1985. "Prediction of Material Damping in Randomly Oriented Short Fiber Polymer Matrix Composites," 4:262-272.
3. Sun, C. T., J. K. Wu and R. F. Gibson. 1987. "Prediction of Material Damping of Laminated Polymer Matrix Composites," *Journal of Material Science*, 22:1006-1012.
4. Sun, C. T., B. V. Sankar and V. S. Rao. 1990. "Damping and Vibration Control of Unidirectional Composite Laminates Using Add-on Viscoelastic Materials," *Journal of Sound and Vibration*, 139(2):277-287.
5. Johnson, C. D., D. A. Kienholz, E. M. Austin and N. E. Schneider. "Finite Element Design of Viscoelastically Damped Structures," *Proceedings of Vibration Damping Workshop, Feb. 27-29, 1984*, pp. HH1-HH8.
6. Ungar, E. E. and E. M. Kerwin, Jr. 1962. "Loss Factors of Viscoelastic Systems in Terms of Energy Concepts," *Journal of Acoustical Society of America*, 24(3):954-957.
7. Bathe, K.-J. 1982. *Finite Element Procedures in Engineering Analysis*. Prentice-Hall.
8. Soni, M. L. and F. K. Bogner. 1982. "Finite Element Vibration Analysis of Damped Structures," *AIAA Journal*, 20(5):700-707.
9. Suarez, S. A. and R. F. Gibson. 1987. "Improved Impulse-Frequency Response Technique for Measurement of Dynamic Mechanical Properties of Composite Materials," *J. of Testing and Evaluation*, 15(2):114-121.
10. Plunkett, R. and C. T. Lee. 1970. "Length Optimization for Constrained Viscoelastic Layer Damping," *Journal of Acoustical Society of America*, 48:151-158.
11. Mantena, P. R. 1989. "Vibration Control of Composite Structural Elements with Constrained Layer Damping Treatments," Doctoral Dissertation, University of Idaho, Moscow, ID.